Broken symmetry in LaAlO$_3$ single crystal probed by resonant Raman spectroscopy

FAST TRACK COMMUNICATION

Broken symmetry in LaAlO$_3$ single crystal probed by resonant Raman spectroscopy

V G Sathe[1] and A Dubey

UGC-DAE Consortium for Scientific Research, University Campus, Khandwa Road, Indore-452017, India

E-mail: vasant@csr.ernet.in

Abstract
Micro-Raman spectra of LaAlO$_3$ single crystal were measured in the temperature range from 90 to 500 K using a 488 and 632.8 nm excitation source. For temperatures other than room temperature and a 488 nm excitation wavelength, the spectra show an additional peak at $\sim$120 cm^{-1} that is not observed for spectra taken with a 632.8 nm excitation wavelength. The extra mode besides the A$_{1g}$ mode implies that the local crystal symmetry is different from the hitherto assumed $R\bar{3}c$ symmetry and can be explained by considering a lack of inversion symmetry with space group $R3c$ or a lack of mirror symmetry with space group $R\bar{3}$.

(Some figures in this article are in colour only in the electronic version)

In the perovskite structure local symmetry plays a very important role in deciding the physical properties [1–3]. Diffraction experiments give a global picture of the space group symmetry and extended absorption spectroscopy (EXAFS) is often used to probe the local symmetry. Optical spectra are known to probe the local symmetry, and in particular the presence of inversion symmetry in a crystal system [4]. Resonant Raman spectroscopy has been a useful tool for probing the local symmetry [5, 6].

LaAlO$_3$ crystallizes in a simple perovskite structure and is widely used as a substrate material for thin film deposition. It shows a rhombohedral to cubic transition when heated above $\sim$800 K [7–10]. This phase transition is attributed to the distortion of oxygen octahedra. In an ideal perovskite (ABO$_3$) cubic structure the B-O6 octahedra are undistorted. In comparison to this ideal cubic structure, structural modifications can be categorized by separating two contributions: (i) a rotation (tilt) of the B-O6 octahedra along some crystallographic direction and (ii) cation (A and/or B) displacements from a mean position [11, 12]. The cubic to rhombohedral transition below 800 K in LaAlO$_3$ is attributed to

---

[1] Author to whom any correspondence should be addressed.

IOP FTC ▶▶▶

J. Phys.: Condens. Matter **19** (2007) 382201   Fast Track Communication

the first category, that is rotation or tilt of the oxygen octahedra along the (111) cubic unit cell direction. This rotation angle serves as an order parameter across the phase transition [10].

Due to their structural similarity and use as substrate materials for growing thin films of colossal magneto-resistance materials like $LaMnO_3$ and doped manganites and other oxides like high-T_c superconductors, dilute magnetic semiconductors etc, attempts were made to compare the room temperature Raman spectra obtained from $LaMnO_3$ and $LaAlO_3$ [13]. However, it was observed that the two compounds exhibit entirely different Raman spectra although they belong to the same structure with space group symmetry $R\bar{3}C$. The difference is attributed to Jahn–Teller distortion-activated modes that are present in $LaMnO_3$ (as observed in $LaMnO_3$ at $\sim$500 and $\sim$610 cm^{-1}) while these are absent in $LaAlO_3$ [13, 14]. In many of the previous reports weak but distinct Raman peaks in the spectra of $LaAlO_3$ that were observed at $\sim$180, 203 and $\sim$467 cm^{-1} were considered as ghost modes [7, 10].

All this prompted us to look again at the temperature evolution of the Raman spectra for $LaAlO_3$. Apart from this, $LaAlO_3$ has been the subject of renewed interest due to its possible use as a high-k dielectric that can offer an alternative to silicon dioxide in complementary metal-oxide semiconductor devices [15]. In this connection knowledge of the optical and crystallographic properties is essential. In this report we show lowering of crystallographic symmetry, as detected by Raman spectroscopy carried out with different excitation wavelengths. It is shown that Raman spectroscopy can be a very sensitive tool for detecting the local symmetry of a crystalline system.

The $LaAlO_3$ single crystal sample was commercially obtained from the MTI Corporation, USA, in the form of a substrate ($10 \times 10 \times 0.5$ mm^3) with one side polished. The substrate was semi-transparent and milky coloured. The surface of the crystal was of [001] orientation with respect to the pseudo cubic unit cell of $LaAlO_3$. The Raman measurements were performed using a LabRam HR 800 Micro-Raman instrument with either a 9 mW HeNe (632.8 nm) or 10 mW Ar (488 nm) laser as an excitation source focused into a $\sim$1 μm diameter spot in a back scattering geometry, where the incident beam is linearly polarized and the spectral detection unpolarized or polarized in the XX and XY direction, where X and Y represent the [100] and [010] directions of the pseudo-cubic unit cell of the $LaAlO_3$ crystal that is perpendicular to the incident beam. A Mplan $50\times$ lens was used during all the measurements and a Peltier cooled CCD for spectral detection. A super notch filter with a lower cut off at 50 cm^{-1} was used for Rayleigh line rejection.

Figures 1(a) and (b) show the unpolarized Raman spectra recorded at 300 and 100 K with excitation wavelengths of 633 and 488 nm, respectively. At room temperature the Raman spectrum of $LaAlO_3$ is characterized by four dominant modes. An E_{1g} soft mode occurring at 34 cm^{-1} (not seen in the present experimental set-up), another soft mode A_{1g} occurring at 125 cm^{-1} and two E_{1g} modes observed around 155 and 488 cm^{-1} [7, 9, 10]. The temperature behaviour of the strongest Raman band (A_{1g}) at $\sim$123 cm^{-1} and that observed at $\sim$151 cm^{-1} are entirely different for the two excitation wavelengths. On the one hand, for the 633 nm excitation wavelength the intensity of the $\sim$123 cm^{-1} band increases marginally while the 151 cm^{-1} band showed a strong increase with decrease in temperature as expected; on the other hand, for the 488 nm excitation wavelength the $\sim$123 cm^{-1} band showed a strong increase with decreasing temperature while the $\sim$151 cm^{-1} band showed a marginal gain in intensity. This complementary behaviour is accompanied by an extra weak Raman band around 120 cm^{-1} appearing below $\sim$240 K for the 488 nm excitation wavelength. This new band became stronger as the temperature is lowered. Figure 2 shows the temperature evolution of the extra Raman band that appeared with the 488 nm excitation wavelength. It is seen that the A_{1g} band, being a soft band, shifts very rapidly with lowering or increasing temperature and hence the newly detected band is seen at the left at low temperature, not seen at all at around room temperature
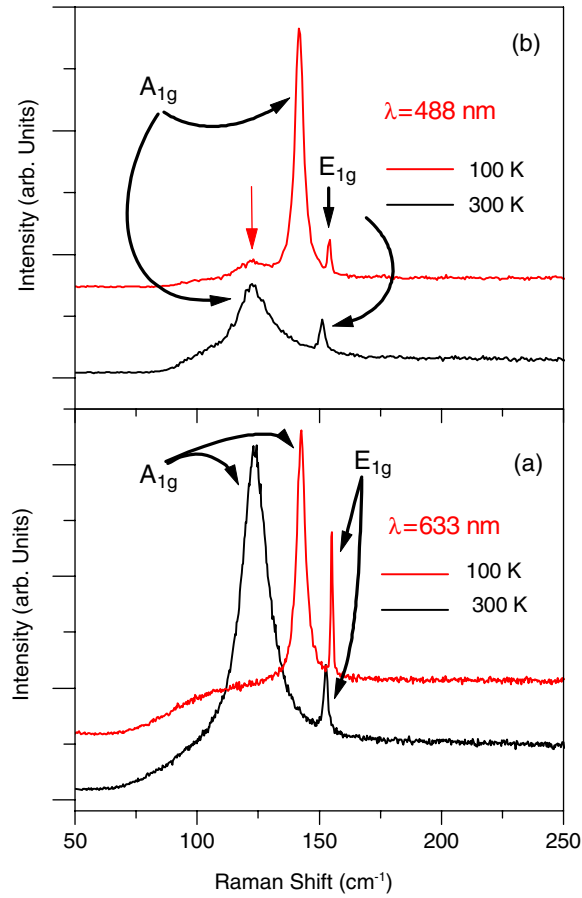
Figure 1. ((a), (b)): The Raman spectra recorded on single crystal LaAlO$_3$ at room temperature (300 K) and 100 K with (a) 632.8 nm excitation source, (b) 488 nm excitation. The straight arrow in (b) depicts the extra mode observed at 100 K.

and is seen as a hump on the right side of the soft A$_{1g}$ mode above room temperature (see inset of figure 2). This shows that the newly observed peak is a separate normal mode that showed normal softening with increase in temperature that can be purely attributed to the lattice expansion effect. This peak is observed in anti-Stokes measurement also, further strengthening its origin as a Raman band. It is also worth noting here that apart from four major Raman bands, few very weak bands are also observed (these are marked by arrows in figure 2) around ∼180, ∼205 and ∼465 cm^{-1} which have been seen by many workers and attributed to ghost modes or non-Raman bands [7, 10, 13]. These modes also showed normal softening with increasing temperature.

The UV–visible spectra shown in figure 3 indicate increased absorption with increasing exciting laser energy and getting close to the resonance condition, though the laser excitation energies (1.96 and 2.55 eV) used in our Raman experiments are still below the absorption jump (3.87 eV) which is a signature of direct electronic transition. The Raman scattering efficiency for a given phonon can be expressed as

$$\frac{\omega_s^4}{c^4} V^2 v \left| \boldsymbol{e}_s \cdot \frac{\mathrm{d}\chi}{\mathrm{d}\xi} \cdot \boldsymbol{e}_L \right|^2$$
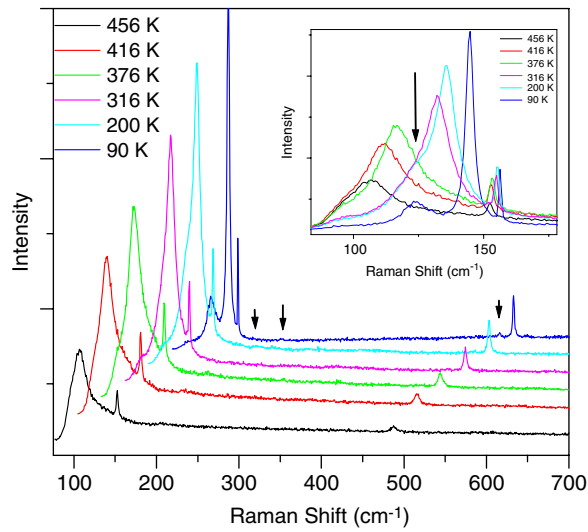
Figure 2. The temperature evolution of Raman spectra recorded from 456 K down to 90 K ($\lambda_L = 488$ nm). The arrows depicts very weak Raman bands. The inset shows the enlarge view of temperature evolution of new Raman band observed as a shoulder on the right side (left side) of the strongest A_1 Raman band at high temperatures (low temperatures).
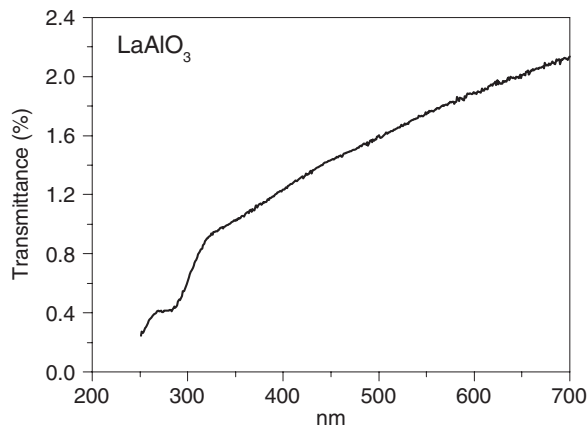

Figure 3. UV–visible spectra of single crystal LaAlO$_3$.

where s and L are indices for *incident* and *scattered* radiation, e_s and e_L represent the incident and scattered polarization, V denotes scattering volume, $\frac{d\chi}{d\xi}$ denotes the Raman tensor, where χ represents the electric susceptibility and ξ the normal coordinates for the optical modes with crystal momentum $\mathbf{q} \cong 0$ [5]. In particular, near a critical point, the non-zero components of $\frac{d\chi}{d\xi}$ may significantly increase due to strong modulation of the combined electronic densities of states (and hence of χ) by particular atomic vibrations. The resonance conditions for LaAlO$_3$ change with variation of the excitation photon energy as manifested by the significant difference of the relative intensity of the 123 and 151 cm^{-1} modes with 632.8 and 488 nm excitation (figure 1). It is also expected from the transmittance spectra shown in figure 3 that the system
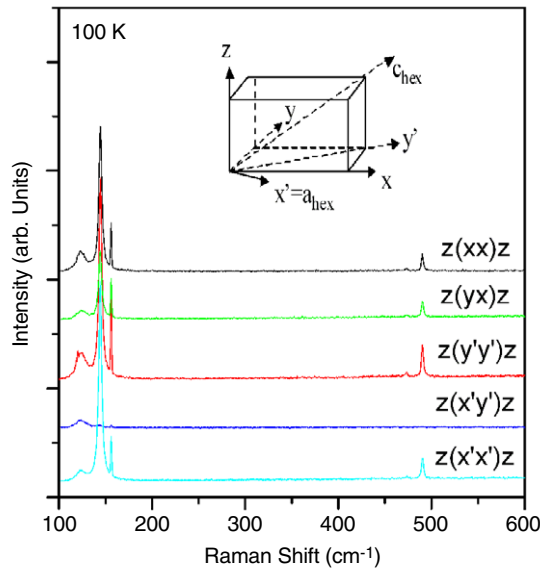
4

IOP FTC ▶▶▶

J. Phys.: Condens. Matter **19** (2007) 382201   Fast Track Communication

Figure 4. Polarized Raman spectra in different scattering configurations obtained from a quasi-cubic [100] surface of LaAlO$_3$ single crystal recorded at 100 K ($\lambda_L = 488$ nm). The inset shows the symbols used for the different crystal directions.

is going closer to the resonance condition, though not very near the critical point, when the 488 nm excitation wavelength is used.

Figure 4 shows the polarization dependence of LaAlO$_3$ crystal recorded in the same manner as described by Abrashev *et al* [13]. The extra resonant peak observed showed polarization dependence concurrent with E$_g$ modes. In order to take care of this extra mode we look back at the phase transition and symmetries of LaAlO$_3$ crystals and the corresponding normal modes deduced from group theory reported so far.

It is known that LaAlO$_3$ shows a phase transition from cubic to rhombohedral symmetry below ∼800 K. In cubic symmetry all the ions occupy a special position and are at the centre of inversion and no Raman band is active by the selection rule. In the rhombohedral structure with space group $R\bar{3}c$, the Al atoms remains at the centre of symmetry while due to distortion in oxygen octahedra around Al atoms, the oxygen and La atoms are no longer at the centre of symmetry. It is known that the degree of tilt of the oxygen octahedra changes as the temperature is lowered due to a reduction in inter-atomic distances. This change in the degree of octahedral distortion lowers the symmetry of the unit cell bringing in the structural phase transition. In order to accommodate the extra normal mode as seen by our present study we look at the other possible space groups similar to $R\bar{3}c$. So long as the transition-metal ion remains a centre of inversion symmetry, three space groups, $R\bar{3}c$, $R\bar{3}m$ and $R\bar{3}$, are possible in the rhombohedral cell containing two molecules. In the space group $R\bar{3}c$, the two aluminium ions are not distinguishable, and the closed-packed oxygen–lanthanum (111) planes remain equidistant from neighbouring (111) aluminium planes. In $R\bar{3}m$, the two aluminium ions per unit cell are not equivalent; the oxygen and lanthanum (111) planes, which coincide in $R\bar{3}c$ symmetry are displaced independently along the c axis. In the space group $R\bar{3}$, neither the c-axis glide nor the mirror symmetry are preserved, and the atomic displacements may be decomposed into an $R\bar{3}c$ component and an $R\bar{3}m$ component. The group theoretical analysis for the LaAlO$_3$ structure with space group $R\bar{3}m$ results in 6(2A$_{1g}$ + 4E$_g$) Raman active modes.

IOP FTC ▶▶▶

J. Phys.: Condens. Matter **19** (2007) 382201   Fast Track Communication

Table 1. Experimental values of the Raman mode frequencies (in cm^{-1}) in the rhombohedral structure (space group $R3C(C_{3v}^6)/R\bar{3}$ (C_{3i}^2)). The last column gives the symmetries of the corresponding mode in the $R\bar{3}C$ (D_{3d}^6) space group.

Expt. Raman	Mode symmetry	Corresponding modes in $R\bar{3}C$
32[a]	E	E_g
123	A_1	A_{1g}
122	E	Not allowed
152	E	E_g
180	A_1	Not allowed
203	A_1	Not allowed
464	E	Not allowed
488	E	E_g

[a] As experimentally observed in [7, 10].

As the number of observed modes is much larger, this seems less probable. Group theoretical analysis for space group $R\bar{3}$ results in $12(4A_{1g} + 4E_{1g} + 4E_{2g})$ Raman active modes.

Another possibility emerges if we consider the lack of inversion symmetry. If one considers that below the phase transition temperature, $LaAlO_3$ shows a lowering of local symmetry to a rhombohedral structure due to tilt/rotation of oxygen octahedra that results in space group $R\bar{3}C$ but also accompanied by a small amount of cation La/Al displacement from the centre of symmetry. Al atoms shift slightly from the centre of inversion, resulting in the $R3c$ space group instead of $R\bar{3}c$. If the shift is very small then the non-centrosymmetric structure ($R3c$) of $LaAlO_3$ differs marginally from its centrosymmetric $R\bar{3}c$ structure, and for each zone centre phonon mode of the latter structure one can have a $R3c$ zone centre counterpart mode involving similar atomic motions. As the $R3c$ space group possesses reduced atomic site symmetry in comparison to $R\bar{3}c$, some of the modes that are Raman inactive in $R\bar{3}c$ become active in $R3c$. Now if the distortion from a centrosymmetric structure is small then it is plausible to expect weak polarizability modulation and hence low Raman intensities for the extra Raman modes that are allowed only because of broken inversion symmetry. These very weak peaks in the Raman spectra can only be detected near Resonance conditions.

Group theoretically it can be shown that the $R\bar{3}c$ space group (D_{3d}^6) rhombohedral unit cell of $LaAlO_3$ gives rise to $27(k = 0)$ optical modes. Out of these only five are Raman active: $A_{1g} + 4E_g$. Abrashev *et al* [13] have given the peak positions of these Raman active modes based on local density of states calculations. When we perform the group theoretical analysis for $R3c$, the zone centre optical modes belonging to the irreducible representations of the group $R3c$ (C_{3v}^6) results in $4A_1 + 4A_2 + 8E$. The $4A_2$ phonons are neither infrared nor Raman active. In the new representation, $12(4A_1 + 8E)$ Raman active modes are allowed against the $5(A_{1g} + 4E_g)$ modes that are Raman active by the representation $R\bar{3}c$. Previously, many workers [7, 10, 13] attributed peaks appearing at 180, 203 and 464 cm^{-1} as ghost modes. In the new symmetry ($R3c$), these modes can also be accommodated in the group theoretical description of the symmetry allowed Raman modes and provides a much more comprehensive explanation of the Raman spectra. A similar argument for the assignment of Raman modes is valid for the space group $R\bar{3}$; the nature of Raman modes being similar $[12(4A_{1g} + 4E_{1g} + 4E_{2g})]$. The nomenclature of the modes in space group $R3c/R\bar{3}$ is given in table 1 along with the corresponding modes in $R\bar{3}c$. Normal diffraction experiments are not expected to detect this lowering of local symmetry resulting from the breakdown of inversion symmetry. It is well known that normal diffraction patterns (x-ray or neutron) from a crystal appear to be centrosymmetric, even when the crystal is non-centrosymmetric. Thus

from the diffraction technique one cannot distinguish between a centrosymmetric and non-centrosymmetric point group and this has the effect of adding a centre of inversion to the point group of the crystal. Again, if the local distortion resulting from oxygen motion is responsible for lowering of the symmetry then it is also highly unlikely to be detected by x-rays. This may be the reason why in diffraction experiments the marginal breakdown of the centre of inversion has not been detected. In order to confirm these findings resonant x-ray diffraction studies are desirable and are planned to be carried out in the future. We believe that these findings will play important role in the actual application of $LaAlO_3$ because even a slight deviation from the centre of symmetry affects the dielectric and related properties. However, in order to clearly bring out the proposed resonance enhancement and observation of extra modes, further Raman measurements with shorter wavelengths, preferably with a UV excitation source, are highly desirable.

In summary, we have investigated the temperature dependence of the optical modes in a high-quality $LaAlO_3$ crystal by means of resonant micro-Raman spectroscopy. For temperatures other than room temperature the spectra for the 488 nm excitation wavelength exhibit an extra mode besides the A_{1g} soft mode; the behaviour was different from that of a single A_{1g} band observed for the 632.8 nm excitation wavelength. Three other weak bands, previously called ghost bands, were also observed. The observation of extra Raman bands is attributed to the local breakdown of symmetry. A space group $R3c/R\bar{3}$ for the compound is proposed at room temperature in the place of $R\bar{3}c$. It is shown that either of these space groups explains the Raman spectra more comprehensively. We argue that the observation of the extra mode could be due to resonance effects that made it possible to probe the small deviation of local symmetry.

References

[1] Grinberg I, Cooper V R and Rappe A M 2002 *Nature* **419** 909
[2] Osada M, Kakihna M, Wada S, Noma T and Cho W-S 1999 *Appl. Phys. Lett.* **75** 3393
[3] Íñiguez J, García A and Perez-Mato J M 2000 *J. Phys.: Condens. Matter* **12** L387
[4] Poulet H and Mathieu J P 1976 *Vibration Spectra and Symmetry of Crystals* (New York: Gordon and Breach)
    Turrell G 1972 *Infrared and Raman Spectra of Crystals* (London: Academic)
[5] Cardona M 1982 *Light Scattering in Solids II* (Berlin: Springer) chapter 2
[6] Long D A 2002 *The Raman Effect: A Unified Treatment of the Theory of Raman Scattering by Molecules* (New York: Wiley)
[7] Scott J F 1969 *Phys. Rev.* **183** 823
[8] Scott J F 1974 *Rev. Mod. Phys.* **46** 83
[9] Muller K A, Berlinger W and Waldner F 1968 *Phys. Rev. Lett.* **21** 814
[10] Hayward S A, Morrison F D, Redfern S A T, Salje E K H, Scott J F, Knight K S, Tarantino S, Glazer A M, Shuvaeva V, Daniel P, Zhang M and Carpenter M A 2005 *Phys. Rev.* B **72** 54110
[11] Glazer A M 1975 *Acta Crystallogr.* A **31** 756
[12] Bouvier P and Kreisel J 2002 *J. Phys.: Condens. Matter* **14** 3981
[13] Abrashev M V, Litvinchuk A P, Iliev M N, Meng R L, Popov V N, Ivanov V G, Chakalov R A and Thomsen C 1999 *Phys. Rev.* B **59** 4146
[14] Iliev M N and Abrashev M V 2001 *J. Raman Spectrosc.* **32** 805
[15] Shevlin S A, Curioni A and Andreoni W 2005 *Phys. Rev. Lett.* **94** 146401